Electronic Transactions on Numerical Analysis.
Volume 37, pp. 386-412, 2010.

ISSN 1068-9613.

ETNA
Kent State University
http://etna.math.kent.edu

A SPECTRAL METHOD FOR THE EIGENVALUE PROBLEM FOR ELLIPTIC EQUATIONS*

KENDALL ATKINSON† AND OLAF HANSEN‡

Abstract. Let Ω be an open, simply connected, and bounded region in $\mathbb{R}^d$, $d \geq 2$, and assume its boundary $\partial\Omega$ is smooth. Consider solving the eigenvalue problem $Lu = \lambda u$ for an elliptic partial differential operator L over Ω with zero values for either Dirichlet or Neumann boundary conditions. We propose, analyze, and illustrate a 'spectral method' for solving numerically such an eigenvalue problem. This is an extension of the methods presented earlier by Atkinson, Chien, and Hansen [Adv. Comput. Math, 33 (2010), pp. 169–189, and to appear].

Key words. elliptic equations, eigenvalue problem, spectral method, multivariable approximation

AMS subject classifications. 65M70

1. Introduction.

We consider the numerical solution of the eigenvalue problem

$$Lu(s) \equiv -\sum_{k,\ell=1}^{d} \frac{\partial}{\partial s_k}\left(a_{k,\ell}(s)\frac{\partial u(s)}{\partial s_\ell}\right) + \gamma(s)u(s) = \lambda u(s), \qquad s \in \Omega \subseteq \mathbb{R}^d, \tag{1.1}$$

with the Dirichlet boundary condition

$$u(s) \equiv 0, \qquad s \in \partial\Omega, \tag{1.2}$$

or with Neumann boundary condition

$$Nu(s) \equiv 0, \qquad s \in \partial\Omega, \tag{1.3}$$

where the conormal derivative $Nu(s)$ on the boundary is given by

$$Nu(s) := \sum_{j,k=1}^{d} a_{j,k}(s)\frac{\partial u}{\partial s_j}\vec{n}_k(s),$$

and $\vec{n}(s)$ is the inside normal to the boundary $\partial\Omega$ at s. Assume $d \geq 2$. Let Ω be an open, simply-connected, and bounded region in $\mathbb{R}^d$, and assume that its boundary $\partial\Omega$ is smooth and sufficiently differentiable. Similarly, assume the functions $\gamma(s)$ and $a_{i,j}(s)$, $1 \leq i, j \leq d$, are several times continuously differentiable over $\overline{\Omega}$. As usual, assume the matrix $A(s) = [a_{i,j}(s)]$ is symmetric and satisfies the strong ellipticity condition,

$$\xi^{\mathrm{T}} A(s)\xi \geq c_0 \xi^{\mathrm{T}}\xi, \qquad s \in \overline{\Omega}, \quad \xi \in \mathbb{R}^d, \tag{1.4}$$

with $c_0 > 0$. For convenience and without loss of generality, we assume $\gamma(s) > 0$, $s \in \Omega$; for otherwise, we can add a multiple of $u(s)$ to both sides of (1.1), shifting the eigenvalues by a known constant.

In the earlier papers [5] and [6], we introduced a spectral method for the numerical solution of elliptic problems over Ω with Dirichlet and Neumann boundary conditions, respectively. In the present work, this spectral method is extended to the numerical solution of

*Received May 27, 2010. Accepted for publication October 14, 2010. Published online December 17, 2010. Recommended by O. Widlund.

†Departments of Mathematics and Computer Science, University of Iowa, Iowa City, IA 52242 (atkinson@divms.uiowa.edu).

‡Department of Mathematics, California State University at San Marcos, San Marcos, CA 92096 (ohansen@csusm.edu).

ETNA
Kent State University
http://etna.math.kent.edu

the eigenvalue problem for (1.1), (1.2) and (1.1), (1.3). We note, again, that our work applies only to regions Ω with a boundary $\partial\Omega$ that is smooth.

There is a large literature on spectral methods for solving elliptic partial differential equations; for example, see the books [10, 11, 12, 17, 26]. The methods presented in these books use a decomposition and/or transformation of the region and problem so as to apply one-variable approximation methods in each spatial variable. In contrast, the present work and that of our earlier papers [5, 6] use multi-variable approximation methods. During the past 20 years, principally, there has been an active development of multi-variable approximation theory, and it is this which we are using in defining and analyzing our spectral methods. It is not clear as to how these new methods compare to the earlier spectral methods, although our approach is rapidly convergent; see Section 4.2 for a numerical comparison. This paper is intended to simply present and illustrate these new methods, with detailed numerical and computational comparisons to earlier spectral methods to follow later.

The numerical method is presented in Section 2, including an error analysis. Implementation of the method is discussed in Section 3 for problems in both $\mathbb{R}^2$ and $\mathbb{R}^3$. Numerical examples are presented in Section 4.

2. The eigenvalue problem. Our spectral method is based on polynomial approximation on the unit ball B_d in $\mathbb{R}^d$. To transform a problem defined on Ω to an equivalent problem defined on B_d, we review some ideas from [5, 6], modifying them as appropriate for this paper.

Assume the existence of a function

$$\Phi : \overline{B}_d \underset{onto}{\overset{1-1}{\longrightarrow}} \overline{\Omega} \tag{2.1}$$

with Φ a twice–differentiable mapping, and let $\Psi = \Phi^{-1} : \overline{\Omega} \underset{onto}{\overset{1-1}{\longrightarrow}} \overline{B}_d$. For $v \in L^2(\Omega)$, let

$$\widetilde{v}(x) = v(\Phi(x)), \qquad x \in \overline{B}_d \subseteq \mathbb{R}^d, \tag{2.2}$$

and conversely,

$$v(s) = \widetilde{v}(\Psi(s)), \qquad s \in \overline{\Omega} \subseteq \mathbb{R}^d. \tag{2.3}$$

Assuming $v \in H^1(\Omega)$, we can show that

$$\nabla_x \widetilde{v}(x) = J(x)^{\mathrm{T}} \nabla_s v(s), \qquad s = \Phi(x),$$

with $J(x)$ the Jacobian matrix for Φ over the unit ball B_d,

$$J(x) \equiv (D\Phi)(x) = \left[\frac{\partial \varphi_i(x)}{\partial x_j}\right]_{i,j=1}^{d}, \qquad x \in \overline{B}_d.$$

To use our method for problems over a region Ω, it is necessary to know explicitly the functions Φ and J. We assume

$$\det J(x) \neq 0, \qquad x \in \overline{B}_d.$$

Similarly,

$$\nabla_s v(s) = K(s)^{\mathrm{T}} \nabla_x \widetilde{v}(x), \qquad x = \Psi(s),$$

with $K(s)$ the Jacobian matrix for Ψ over Ω. By differentiating the identity

$$\Psi(\Phi(x)) = x, \qquad x \in \overline{B}_d,$$

ETNA
Kent State University
http://etna.math.kent.edu

we obtain

$$K\left(\Phi\left(x\right)\right) = J\left(x\right)^{-1}.$$

Assumptions about the differentiability of $\widetilde{v}\left(x\right)$ can be related back to assumptions on the differentiability of $v(s)$ and $\Phi(x)$.

LEMMA 2.1. *If* $\Phi \in C^k\left(\overline{B}_d\right)$ *and* $v \in C^m\left(\overline{\Omega}\right)$, *then* $\widetilde{v} \in C^q\left(\overline{B}_d\right)$ *with* $q = \min\{k, m\}$.

Proof. A proof is straightforward using (2.2). □

A converse statement can be made as regards $\widetilde{v}$, v, and Ψ in (2.3).

Consider now the nonhomogeneous problem $Lu = f$,

$$Lu(s) \equiv -\sum_{k,\ell=1}^{d} \frac{\partial}{\partial s_k}\left(a_{k,\ell}(s)\frac{\partial u(s)}{\partial s_\ell}\right) + \gamma(s)u(s) = f(s), \qquad s \in \Omega \subseteq \mathbb{R}^d. \tag{2.4}$$

Using the transformation (2.1), it is shown in [5, Thm 2] that (2.4) is equivalent to

$$\begin{aligned} -\sum_{k,\ell=1}^{d} \frac{\partial}{\partial x_k}\left(\widetilde{a}_{k,\ell}(x)\det\left(J(x)\right)\frac{\partial \widetilde{v}(x)}{\partial x_\ell}\right) + \left[\widetilde{\gamma}(x)\det J(x)\right]\widetilde{u}(x) \\ = \widetilde{f}\left(x\right)\det J(x), \qquad x \in B_d, \end{aligned}$$

with the matrix $\widetilde{A}\left(x\right) \equiv \left[\widetilde{a}_{i,j}(x)\right]$ given by

$$\widetilde{A}\left(x\right) = J\left(x\right)^{-1} A\left(\Phi\left(x\right)\right) J\left(x\right)^{-\mathrm{T}}. \tag{2.5}$$

The matrix $\widetilde{A}$ satisfies the analogue of (1.4), but over B_d. Thus the original eigenvalue problem (1.1) can be replaced by

$$\begin{aligned} -\sum_{k,\ell=1}^{d} \frac{\partial}{\partial x_k}\left(\widetilde{a}_{k,\ell}(x)\det\left(J(x)\right)\frac{\partial \widetilde{u}(x)}{\partial x_\ell}\right) + \left[\widetilde{\gamma}(x)\det J(x)\right]\widetilde{u}(x) \\ = \lambda\widetilde{u}(x)\det J(x), \qquad x \in B_d. \end{aligned} \tag{2.6}$$

As a consequence of this transformation, we can work with an elliptic problem defined over B_d rather than over the original region Ω. In the following we will use the notation L_D and L_N when we like to emphasize the domain of the operator L, so

$$\begin{aligned} L_D &: H^2(\Omega) \cap H_0^1(\Omega) \to L^2(\Omega) \\ L_N &: H_N^2(\Omega) \to L^2(\Omega) \end{aligned}$$

are invertible operators; see [21, 28]. Here $H_N^2(\Omega)$ is defined by

$$H_N^2(\Omega) = \{u \in H^2(\Omega) : Nu(s) = 0,\ s \in \partial\Omega\}.$$

2.1. The variational framework for the Dirichlet problem. To develop our numerical method, we need a variational framework for (2.4) with the Dirichlet condition $u = 0$ on $\partial\Omega$. As usual, multiply both sides of (2.4) by an arbitrary $v \in H_0^1\left(\Omega\right)$, integrate over Ω, and apply integration by parts. This yields the problem of finding $u \in H_0^1\left(\Omega\right)$ such that

$$\mathcal{A}\left(u, v\right) = \left(f, v\right) \equiv \ell\left(v\right), \qquad \text{for all } v \in H_0^1\left(\Omega\right), \tag{2.7}$$

ETNA
Kent State University
http://etna.math.kent.edu

with

$$\mathcal{A}(v,w) = \int_\Omega \left[\sum_{k,\ell=1}^{d} a_{k,\ell}(s) \frac{\partial v(s)}{\partial s_\ell} \frac{\partial w(s)}{\partial s_k} + \gamma(s) v(s) w(s) \right] ds, \quad v, w \in H_0^1(\Omega). \tag{2.8}$$

The right side of (2.7) uses the inner product $(\cdot,\cdot)$ of $L^2(\Omega)$. The operators L_D and $\mathcal{A}$ are related by

$$(L_D u, v) = \mathcal{A}(u,v), \qquad u \in H^2(\Omega), \quad v \in H_0^1(\Omega), \tag{2.9}$$

an identity we use later. The function $\mathcal{A}$ is an inner product and it satisfies

$$|\mathcal{A}(v,w)| \le c_{\mathcal{A}} \|v\|_1 \|w\|_1, \qquad v, w \in H_0^1(\Omega), \tag{2.10}$$

$$\mathcal{A}(v,v) \ge c_e \|v\|_1^2, \qquad v \in H_0^1(\Omega), \tag{2.11}$$

for some positive constants $c_{\mathcal{A}}$ and c_e. Here the norm $\|\cdot\|_1$ is given by

$$\|u\|_1^2 := \int_\Omega \left[\sum_{k=1}^{d} \left(\frac{\partial u(s)}{\partial s_k} \right)^2 + u^2(s) \right] ds. \tag{2.12}$$

Associated with the Dirichlet problem

$$L_D u(s) = f(s), \qquad x \in \Omega, \quad f \in L^2(\Omega), \tag{2.13}$$

$$u(s) = 0, \qquad x \in \partial\Omega, \tag{2.14}$$

is the Green's function integral operator

$$u(s) = \mathcal{G}_D f(s). \tag{2.15}$$

LEMMA 2.2. *The operator $\mathcal{G}_D$ is a bounded and self–adjoint operator from $L^2(\Omega)$ into $H^2(\Omega) \cap H_0^1(\Omega)$. Moreover, it is a compact operator from $L^2(\Omega)$ into $H_0^1(\Omega)$, and more particularly, it is a compact operator from $H_0^1(\Omega)$ into $H_0^1(\Omega)$.*

Proof. A proof can be based on [15, Sec. 6.3, Thm. 5] together with the fact that the embedding of $H^2(\Omega) \cap H_0^1(\Omega)$ into $H_0^1(\Omega)$ is compact. The symmetry follows from the self–adjointness of the original problem (2.13)–(2.14). □

We convert (2.9) to

$$(f, v) = \mathcal{A}(\mathcal{G}_D f, v), \qquad v \in H_0^1(\Omega), \quad f \in L^2(\Omega). \tag{2.16}$$

The problem (2.13)–(2.14) has the following variational reformulation: find $u \in H_0^1(\Omega)$ such that

$$\mathcal{A}(u,v) = \ell(v), \qquad \forall v \in H_0^1(\Omega). \tag{2.17}$$

This problem can be shown to have a unique solution u by using the Lax–Milgram Theorem to imply its existence; see [8, Thm. 8.3.4]. In addition,

$$\|u\|_1 \le \frac{1}{c_e} \|\ell\|$$

with $\|\ell\|$ denoting the operator norm for ℓ regarded as a linear functional on $H_0^1(\Omega)$.

ETNA
Kent State University
http://etna.math.kent.edu

2.2. The variational framework for the Neumann problem. Now we present the variational framework for (2.4) with the Neumann condition $Nu = 0$ on $\partial\Omega$. Assume that $u \in H^2(\Omega)$ is a solution to the problem (2.4),(1.3). Again, multiply both sides of (2.4) by an arbitrary $v \in H^1(\Omega)$, integrate over Ω, and apply integration by parts. This yields the problem of finding $u \in H^1(\Omega)$ such that

$$\mathcal{A}(u,v) = (f,v) \equiv \ell(v), \qquad \text{for all } v \in H^1(\Omega), \tag{2.18}$$

with $\mathcal{A}$ given by (2.8).The right side of (2.18) uses again the inner product of $L^2(\Omega)$. The operators L_N and $\mathcal{A}$ are now related by

$$(L_N u, v) = \mathcal{A}(u,v), \qquad v \in H^1(\Omega), \tag{2.19}$$

and $u \in H^2(\Omega)$ which fulfills $Nu \equiv 0$. The inner product $\mathcal{A}$ satisfies the properties (2.10) and (2.11) for functions $u, v \in H^1(\Omega)$.

Associated with the Neumann problem

$$L_N u(s) = f(s), \qquad x \in \Omega, \quad f \in L^2(\Omega), \tag{2.20}$$

$$Nu(s) = 0, \qquad x \in \partial\Omega, \tag{2.21}$$

is the Green's function integral operator

$$u(s) = \mathcal{G}_N f(s).$$

LEMMA 2.3. *The operator $\mathcal{G}_N$ is a bounded and self–adjoint operator from $L^2(\Omega)$ into $H^2(\Omega)$. Moreover, it is a compact operator from $L^2(\Omega)$ into $H^1(\Omega)$, and more particularly, it is a compact operator from $H^1(\Omega)$ into $H^1(\Omega)$.*

Proof. The proof uses the same arguments as the proof of Lemma 2.2. □

We convert (2.19) to

$$(f,v) = \mathcal{A}(\mathcal{G}_N f, v), \qquad v \in H^1(\Omega), \quad f \in L^2(\Omega).$$

The problem (2.20)–(2.21) has the following variational reformulation: find $u \in H^1(\Omega)$ such that

$$\mathcal{A}(u,v) = \ell(v), \qquad \forall v \in H^1(\Omega). \tag{2.22}$$

This problem can be shown to have a unique solution u by using the Lax–Milgram Theorem to imply its existence; see [8, Thm. 8.3.4]. In addition,

$$\|u\|_1 \le \frac{1}{c_e}\|\ell\|$$

with $\|\ell\|$ denoting the operator norm for ℓ regarded as a linear functional on $H^1(\Omega)$.

2.3. The approximation scheme. Denote by Π_n the space of polynomials in d variables that are of degree $\le n$: $p \in \Pi_n$ if it has the form

$$p(x) = \sum_{|i|\le n} a_i x_1^{i_1} x_2^{i_2} \dots x_d^{i_d},$$

with i a multi–integer, $i = (i_1, \dots, i_d)$, and $|i| = i_1 + \cdots + i_d$. Over B_d, our approximation subspace for the Dirichlet problem is

$$\widetilde{\mathcal{X}}_{D,n} = \left\{ \left(1 - \|x\|_2^2\right) p(x) \mid p \in \Pi_n \right\},$$

ETNA
Kent State University
http://etna.math.kent.edu

with $\|x\|_2^2 = x_1^2 + \cdots + x_d^2$. The approximation subspace for the Neumann problem is

$$\widetilde{\mathcal{X}}_{\mathcal{N},n} = \Pi_n.$$

(We use here $\mathcal{N}$ to make a distinction between the dimension of $\widetilde{\mathcal{X}}_{\mathcal{N},n}$; see below, and the notation for the subspace.) The subspaces $\widetilde{\mathcal{X}}_{\mathcal{N},n}$ and $\widetilde{\mathcal{X}}_{D,n}$ have dimension

$$N \equiv N_n = \binom{n+d}{d}.$$

However our problem (2.7) is defined over Ω, and thus we use modifications of $\widetilde{\mathcal{X}}_{D,n}$ and $\widetilde{\mathcal{X}}_{\mathcal{N},n}$,

$$\begin{aligned} \mathcal{X}_{D,n} &= \left\{ \psi(s) = \widetilde{\psi}(\Psi(s)) : \widetilde{\psi} \in \widetilde{\mathcal{X}}_{D,n} \right\} \subseteq H_0^1(\Omega), \\ \mathcal{X}_{\mathcal{N},n} &= \left\{ \psi(s) = \widetilde{\psi}(\Psi(s)) : \widetilde{\psi} \in \widetilde{\mathcal{X}}_{\mathcal{N},n} \right\} \subseteq H^1(\Omega). \end{aligned} \tag{2.23}$$

In the following, we avoid the index D and $\mathcal{N}$ if a statement applies to either of the subspaces and write just $\widetilde{\mathcal{X}}_n$ and similarly $\mathcal{X}_n$. This set of functions $\mathcal{X}_n$ is used in the initial definition of our numerical scheme and for its convergence analysis; but the simpler space $\widetilde{\mathcal{X}}_n$ is used in the actual implementation of the method. They are two aspects of the same numerical method.

To solve (2.17) or (2.22) approximately, we use the Galerkin method with trial space $\mathcal{X}_n$ to find $u_n \in \mathcal{X}_n$ for which

$$\mathcal{A}(u_n, v) = \ell(v), \qquad \forall v \in \mathcal{X}_n.$$

For the eigenvalue problem (1.1), find $u_n \in \mathcal{X}_n$ for which

$$\mathcal{A}(u_n, v) = \lambda(u_n, v), \qquad \forall v \in \mathcal{X}_n. \tag{2.24}$$

Write

$$u_n(s) = \sum_{j=1}^{N} \alpha_j \psi_j(s) \tag{2.25}$$

with $\{\psi_j\}_{j=1}^N$ a basis of $\mathcal{X}_n$. Then (2.24) becomes

$$\sum_{j=1}^{N} \alpha_j \mathcal{A}(\psi_j, \psi_i) = \lambda \sum_{j=1}^{N} \alpha_j (\psi_j, \psi_i), \quad i = 1, \ldots, N. \tag{2.26}$$

The coefficients can be related back to a polynomial basis for $\widetilde{\mathcal{X}}_n$ and to integrals over B_d. Let $\left\{\widetilde{\psi}_j\right\}$ denote the basis of $\widetilde{\mathcal{X}}_n$ corresponding to the basis $\{\psi_j\}$ for $\mathcal{X}_n$. Using the transformation $s = \Phi(x)$,

$$\begin{aligned} (\psi_j, \psi_i) &= \int_\Omega \psi_j(s)\, \psi_i(s)\, ds \\ &= \int_{B_d} \widetilde{\psi}_j(x)\, \widetilde{\psi}_i(x)\, |\det J(x)|\, dx, \end{aligned}$$

ETNA
Kent State University
http://etna.math.kent.edu

$$\begin{aligned}
\mathcal{A}(\psi_j,\psi_i) &= \int_\Omega \left[\sum_{k,\ell=1}^{d} a_{k,\ell}(s)\,\frac{\partial\psi_j(s)}{\partial s_k}\frac{\partial\psi_i(s)}{\partial s_\ell} + \gamma(s)\psi_j(s)\psi_i(s)\right] ds \\
&= \int_\Omega \left[\{\nabla_s\psi_i(s)\}^{\mathrm{T}} A(s)\{\nabla_s\psi_j(s)\} + \gamma(s)\psi_j(s)\psi_i(s)\right] ds \\
&= \int_\Omega \left[\left\{K(\Phi(x))^{\mathrm{T}}\nabla_x\widetilde{\psi}_i(x)\right\}^{\mathrm{T}} A(\Phi(x))\left\{K(\Phi(x))^{\mathrm{T}}\nabla_x\widetilde{\psi}_j(x)\right\}\right. \\
&\qquad \left. +\widetilde{\gamma}(x)\widetilde{\psi}_j(x)\widetilde{\psi}_i(x)\right] |\det J(x)|\,dx \\
&= \int_{B_d} \left[\nabla_x\widetilde{\psi}_i(x)^{\mathrm{T}}\,\widetilde{A}(x)\nabla_x\widetilde{\psi}_j(x) + \widetilde{\gamma}(x)\widetilde{\psi}_i(x)\,\widetilde{\psi}_j(x)\right] |\det J(x)|\,dx,
\end{aligned}$$

with the matrix $\widetilde{A}(x)$ given in (2.5). With these evaluations of the coefficients, it is straightforward to show that (2.26) is equivalent to a Galerkin method for (2.6) using the standard inner product of $L^2(B_d)$ and the approximating subspace $\widetilde{\mathcal{X}}_n$.

2.4. Convergence analysis. In this section we will use $\mathcal{G}$ to refer to either of the Green operators $\mathcal{G}_D$ or $\mathcal{G}_N$. In both cases $\mathcal{G}$ is a compact operator from a subspace $\mathcal{Y}\subset L^2(\Omega)$ into itself. We have $\mathcal{Y}=H_0^1(\Omega)$ in the Dirichlet case and $\mathcal{Y}=H^1(\Omega)$ in the Neumann case. In both cases $\mathcal{Y}$ carries the norm $\|\cdot\|_{H^1(\Omega)}$. On B_d we use notation $\widetilde{\mathcal{Y}}$ to denote either of the subspaces $H_0^1(B_d)$ or $H^1(B_d)$ The scheme (2.26) is implicitly a numerical approximation of the integral equation eigenvalue problem

$$\lambda\mathcal{G}u = u. \tag{2.27}$$

LEMMA 2.4. *The numerical method (2.24) is equivalent to the Galerkin method approximation of the integral equation (2.27), with the Galerkin method based on the inner product $\mathcal{A}(\cdot,\cdot)$ for $\mathcal{Y}$.*

Proof. For the Galerkin solution of (2.27) we seek a function u_n in the form (2.25), and we force the residual to be orthogonal to $\mathcal{X}_n$. This leads to

$$\lambda\sum_{j=1}^{N}\alpha_j\mathcal{A}(\mathcal{G}\psi_j,\psi_i) = \sum_{j=1}^{N}\alpha_j\mathcal{A}(\psi_j,\psi_i) \tag{2.28}$$

for $i=1,\ldots,N$. From (2.16), we have $\mathcal{A}(\mathcal{G}\psi_j,\psi_i)=(\psi_j,\psi_i)$, and thus

$$\lambda\sum_{j=1}^{N}\alpha_j(\psi_j,\psi_i) = \sum_{j=1}^{N}\alpha_j\mathcal{A}(\psi_j,\psi_i).$$

This is exactly the same as (2.26). ∎

Let $\mathcal{P}_n$ be the orthogonal projection of $\mathcal{Y}$ onto $\mathcal{X}_n$, based on the inner product $\mathcal{A}(\cdot,\cdot)$. Then (2.28) is the Galerkin approximation,

$$\mathcal{P}_n\mathcal{G}u_n = \frac{1}{\lambda}u_n, \quad u_n\in\mathcal{X}_n, \tag{2.29}$$

for the integral equation eigenvalue problem (2.27). Much is known about such schemes, as we discuss below. The conversion of the eigenvalue problem (2.24) into the equivalent eigenvalue problem (2.29) is motivated by a similar idea used in Osborn [24].

The numerical solution of eigenvalue problems for compact integral operators has been studied by many people for over a century. With Galerkin methods, we note particularly the

ETNA
Kent State University
http://etna.math.kent.edu

early work of Krasnoselskii [20, p. 178]. The book of Chatelin [13] presents and summarizes much of the literature on the numerical solution of such eigenvalue problems for compact operators. For our work we use the results given in [2, 3] for pointwise convergent operator approximations that are collectively compact.

We begin with some preliminary lemmas.

LEMMA 2.5. *For suitable positive constants c_1 and c_2,*

$$c_1\|\widetilde{v}\|_{H^1(B_d)} \le \|v\|_{H^1(\Omega)} \le c_2\|\widetilde{v}\|_{H^1(B_d)}$$

for all functions $v \in \mathcal{Y}$, with $\widetilde{v}$ the corresponding function of (2.2). Thus, for a sequence $\{v_n\}$ in $\mathcal{Y}$,

$$v_n \to v \quad \text{in } \mathcal{Y} \iff \widetilde{v}_n \to \widetilde{v} \quad \text{in } \widetilde{\mathcal{Y}},$$

with $\{\widetilde{v}_n\}$ the corresponding sequence in $\widetilde{\mathcal{Y}}$.

Proof. Begin by noting that there is a 1-1 correspondence between $\mathcal{Y}$ and $\widetilde{\mathcal{Y}}$ based on using (2.1)–(2.3). Next,

$$\begin{aligned}
\|v\|^2_{H^1(\Omega)} &= \int_\Omega \left[|\nabla v\,(s)|^2 + |v(s)|^2\right] ds \\
&= \int_{B_d} \left[\left|\nabla\widetilde{v}\,(x)^{\mathrm{T}}\, J\,(x)^{-1}\, J\,(x)^{-\mathrm{T}}\, \nabla\widetilde{v}\,(x)\right| + |\widetilde{v}(x)|^2\right] |\det J(x)|\; dx \\
&\le \left[\max_{x\in B}|\det J(x)|\right] \max\left\{\max_{x\in B}\|J\,(x)^{-1}\,\|^2, 1\right\} \int_{B_d}\left[|\nabla\widetilde{v}\,(x)|^2 + |\widetilde{v}(x)|^2\right] dx,
\end{aligned}$$

$$\|v\|_{H^1(\Omega)} \le c_2\|\widetilde{v}\|_{H^1(B_d)},$$

for a suitable constant $c_2\,(\Omega)$. The reverse inequality, with the roles of $\|\widetilde{v}\|_{H^1(B_d)}$ and $\|v\|_{H^1(\Omega)}$ reversed, follows by an analogous argument. ∎

LEMMA 2.6. *The set $\cup_{n\ge1}\mathcal{X}_n$ is dense in $\mathcal{Y}$.*

Proof. The set $\cup_{n\ge1}\widetilde{\mathcal{X}}_n$ is dense in $\widetilde{\mathcal{Y}}$, a result shown in [5, see (15)]. We can then use the correspondence between $H\,(\Omega)$ and $H^1\,(B_d)$, given in Lemma 2.5, to show that $\cup_{n\ge1}\mathcal{X}_n$ is dense in $\mathcal{Y}$. ∎

LEMMA 2.7. *The standard norm $\|\cdot\|_1$ on $\mathcal{Y}$ and the norm $\|v\|_{\mathcal{A}} = \sqrt{\mathcal{A}\,(v,v)}$ are equivalent in the topology they generate. More precisely,*

$$\sqrt{c_e}\|v\|_1 \le \|v\|_{\mathcal{A}} \le \sqrt{c_{\mathcal{A}}}\|v\|_1, \qquad v \in \mathcal{Y}, \tag{2.30}$$

with the constants $c_{\mathcal{A}}$, c_e taken from (2.10) and (2.11), respectively. Convergence of sequences $\{v_n\}$ is equivalent in the two norms.

Proof. It is immediate from (2.11) and (2.10). ∎

LEMMA 2.8. *For the orthogonal projection operator $\mathcal{P}_n$,*

$$\mathcal{P}_n v \to v \qquad \text{as} \quad n\to\infty, \qquad \text{for all } v \in \mathcal{Y}. \tag{2.31}$$

Proof. This follows from the definition of an orthogonal projection operator and using the result that $\cup_{n\ge1}\mathcal{X}_n$ is dense in $\mathcal{Y}$. ∎

COROLLARY 2.9. *For the integral operator $\mathcal{G}$,*

$$\|(I-\mathcal{P}_n)\,\mathcal{G}\| \to 0 \quad \text{as} \quad n\to\infty,$$

ETNA
Kent State University
http://etna.math.kent.edu

using the norm for operators from $\mathcal{Y}$ into $\mathcal{Y}$.

Proof. Consider $\mathcal{G}$ and $\mathcal{P}_n$ as operators on $\mathcal{Y}$ into $\mathcal{Y}$. The result follows from the compactness of $\mathcal{G}$ and the pointwise convergence in (2.31); see [4, Lemma 3.1.2]. □

LEMMA 2.10. *$\{\mathcal{P}_n\mathcal{G}\}$ is collectively compact on $\mathcal{Y}$.*

Proof. This follows for all such families $\{\mathcal{P}_n\mathcal{G}\}$ with $\mathcal{G}$ compact on a Banach space $\mathcal{Y}$ and $\{\mathcal{P}_n\}$ pointwise convergent on $\mathcal{Y}$. To prove this requires showing

$$\{\mathcal{P}_n\mathcal{G}v \mid \|v\|_1 \leq 1,\, n \geq 1\}$$

has compact closure in $\mathcal{Y}$. This can be done by showing that the set is totally bounded. We omit the details of the proof. □

Summarizing, $\{\mathcal{P}_n\mathcal{G}\}$ is a collectively compact family that is pointwise convergent on $\mathcal{Y}$. With this, the results in [2, 3] can be applied to (2.29) as a numerical approximation to the eigenvalue problem (2.27). We summarize the application of those results to (2.29).

THEOREM 2.11. *Let λ be an eigenvalue for the problem Dirichlet problem (1.1), (1.2) or the Neumann problem (1.1), (1.3). Assume λ has multiplicity ν, and let $\chi^{(1)}, \ldots, \chi^{(\nu)}$ be a basis for the associated eigenfunction subspace. Let $\varepsilon > 0$ be chosen such that there are no other eigenvalues within a distance ε of λ. Let σ_n denote the eigenvalue solutions of (2.24) that are within ε of λ. Then for all sufficiently large n, say $n \geq n_0$, the sum of the multiplicities of the approximating eigenvalues within σ_n equals ν. Moreover,*

$$\max_{\lambda_n \in \sigma_n} |\lambda - \lambda_n| \leq c \max_{1 \leq k \leq \nu} \| (I - \mathcal{P}_n)\, \chi^{(k)} \|_1. \tag{2.32}$$

Let u be an eigenfunction for λ. Let $\mathcal{W}_n$ be the direct sum of the eigenfunction subspaces associated with the eigenvalues $\lambda_n \in \sigma_n$, and let $\left\{u_n^{(1)}, \ldots, u_n^{(\nu)}\right\}$ be a basis for $\mathcal{W}_n$. Then there is a sequence

$$u_n = \sum_{k=1}^{\nu} \alpha_{n,k} u_n^{(k)} \in \mathcal{W}_n$$

for which

$$\|u - u_n\|_1 \leq c \max_{1 \leq k \leq \nu} \| (I - \mathcal{P}_n)\, \chi^{(k)} \|_1 \tag{2.33}$$

for some constant $c > 0$ dependent on λ.

Proof. . This is a direct consequence of results in [2, 3], together with the compactness of $\mathcal{G}$ on $\mathcal{Y}$. It also uses the equivalence of norms given in (2.30). □

The norms $\| (I - \mathcal{P}_n)\, \chi^{(k)} \|_1$ can be bounded using results from Ragozin [25], just as was done in [5]. We begin with the following result from [25].

LEMMA 2.12. *Assume $w \in C^{k+2}\left(\overline{B}_d\right)$ for some $k > 0$, and assume $w|_{\partial B_d} = 0$. Then there is a polynomial $q_n \in \widetilde{\mathcal{X}}_{D,n}$ for which*

$$\|w - q_n\|_\infty \leq D\,(k,d)\, n^{-k} \left(n^{-1} \|w\|_{\infty,k+2} + \omega\left(w^{(k+2)}, 1/n\right)\right).$$

Here, we have

$$\|w\|_{\infty,k+2} = \sum_{|i| \leq k+2} \left\|\partial^i w\right\|_\infty, \qquad \omega\,(g,\delta) = \sup_{|x-y| \leq \delta} |g\,(x) - g\,(y)|\,,$$

$$\omega\left(w^{(k+2)}, \delta\right) = \sum_{|i| = k+2} \omega\left(\partial^i w, \delta\right).$$

ETNA
Kent State University
http://etna.math.kent.edu

The corresponding result that is needed with the Neumann problem can be obtained from [9].

LEMMA 2.13. *Assume* $w \in C^{k+2}\left(\overline{B}_d\right)$ *for some* $k > 0$. *Then there is a polynomial* $q_n \in \widetilde{\mathcal{X}}_{\mathcal{N},n}$ *for which*

$$\|w - q_n\|_\infty \leq D\,(k,d)\,n^{-k}\left(n^{-1}\,\|w\|_{\infty,k+2} + \omega\left(w^{(k+2)}, 1/n\right)\right).$$

THEOREM 2.14. *Recall the notation and assumptions of Theorem 2.11. Assume the eigenfunction basis functions* $\chi^{(k)} \in C^{m+2}(\Omega)$ *and assume* $\Phi \in C^{m+2}(B_d)$, *for some* $m \geq 1$. *Then*

$$\max_{\lambda_n \in \sigma_n} |\lambda - \lambda_n| = \mathcal{O}\left(n^{-m}\right), \qquad \|u - u_n\|_1 = \mathcal{O}\left(n^{-m}\right).$$

Proof. Begin with (2.32)–(2.33). To obtain the bounds for $\|\,(I - \mathcal{P}_n)\,u^{(k)}\|_1$ given above using Lemma 2.12 or 2.13 , refer to the argument given in [5]. □

3. Implementation. In this section, we use again the notation $\mathcal{X}_n$ if a statement applies to both $\mathcal{X}_{D,n}$ or $\mathcal{X}_{\mathcal{N},n}$; and similarly for $\widetilde{\mathcal{X}}_n$. Consider the implementation of the Galerkin method of (2.24) for the eigenvalue problem (1.1). We are to find the function $u_n \in \mathcal{X}_n$ satisfying (2.26). To do so, we begin by selecting a basis for Π_n that is orthonormal in $L^2(B_d)$, denoting it by $\{\widetilde{\varphi}_1, \ldots, \widetilde{\varphi}_N\}$, with $N \equiv N_n = \dim \Pi_n$. Choosing such an orthonormal basis is an attempt to have the matrix associated with the left side of the linear system in (2.26) be better conditioned. Next, let

$$\widetilde{\psi}_i(\mathbf{x}) = \widetilde{\varphi}_i(\mathbf{x}), \qquad i = 1, \ldots, N_n,$$

in the Neumann case and

$$\widetilde{\psi}_i(\mathbf{x}) = \left(1 - \|\mathbf{x}\|_2^2\right)\widetilde{\varphi}_i(\mathbf{x}), \qquad i = 1, \ldots, N_n, \tag{3.1}$$

in the Dirichlet case. These functions form a basis for $\widetilde{\mathcal{X}}_n$. As in (2.23), use as the corresponding basis of $\mathcal{X}_n$ the set $\{\psi_1, \ldots, \psi_N\}$.

We seek

$$u_n(\mathbf{s}) = \sum_{j=1}^{N} \alpha_j \psi_j(\mathbf{s}).$$

Then following the change of variable $\mathbf{s} = \Phi(\mathbf{x})$, (2.26) becomes

$$\begin{aligned} &\sum_{j=1}^{N} \alpha_j \int_{B_d} \left[\nabla \widetilde{\psi}_j(\mathbf{x})^{\mathrm{T}}\, \widetilde{A}(\mathbf{x}) \nabla \widetilde{\psi}_i(\mathbf{x}) + \widetilde{\gamma}(\mathbf{x}) \widetilde{\psi}_j(\mathbf{x})\, \widetilde{\psi}_i(\mathbf{x})\right] |\det J(\mathbf{x})|\, d\mathbf{x} \\ &\qquad = \lambda \sum_{j=1}^{N} \alpha_j \int_{B_d} \widetilde{\psi}_j(\mathbf{x})\, \widetilde{\psi}_i(\mathbf{x})\, |\det J(\mathbf{x})|\, d\mathbf{x}, \qquad i = 1, \ldots, N. \end{aligned} \tag{3.2}$$

We need to calculate the orthonormal polynomials and their first partial derivatives; and we also need to approximate the integrals in the linear system. For an introduction to the topic of multivariate orthogonal polynomials, see Dunkl and Xu [14] and Xu [29]. For multivariate quadrature over the unit ball in $\mathbb{R}^d$, see Stroud [27].

ETNA
Kent State University
http://etna.math.kent.edu

3.1. The planar case. The dimension of Π_n is

$$N_n = \frac{1}{2}(n+1)(n+2)$$

For notation, we replace $\mathbf{x}$ with (x, y). How do we choose the orthonormal basis $\{\widetilde{\varphi}_\ell(x,y)\}_{\ell=1}^N$ for Π_n? Unlike the situation for the single variable case, there are many possible orthonormal bases over $B = D$, the unit disk in $\mathbb{R}^2$. We have chosen one that is particularly convenient for our computations. These are the "ridge polynomials" introduced by Logan and Shepp [22] for solving an image reconstruction problem. We summarize here the results needed for our work.

Let

$$\mathcal{V}_n = \{P \in \Pi_n : (P, Q) = 0 \quad \forall Q \in \Pi_{n-1}\},$$

the polynomials of degree n that are orthogonal to all elements of Π_{n-1}. Then the dimension of $\mathcal{V}_n$ is $n+1$; moreover,

$$\Pi_n = \mathcal{V}_0 \oplus \mathcal{V}_1 \oplus \cdots \oplus \mathcal{V}_n. \tag{3.3}$$

It is standard to construct orthonormal bases of each $\mathcal{V}_n$ and to then combine them to form an orthonormal basis of Π_n using the latter decomposition. As an orthonormal basis of $\mathcal{V}_n$ we use

$$\widetilde{\varphi}_{n,k}(x,y) = \frac{1}{\sqrt{\pi}} U_n(x\cos(kh) + y\sin(kh)), \quad (x,y) \in D, \quad h = \frac{\pi}{n+1}, \tag{3.4}$$

for $k = 0, 1, \ldots, n$. The function U_n is the Chebyshev polynomial of the second kind of degree n,

$$U_n(t) = \frac{\sin(n+1)\theta}{\sin\theta}, \qquad t = \cos\theta, \quad -1 \le t \le 1, \quad n = 0, 1, \ldots.$$

The family $\{\widetilde{\varphi}_{n,k}\}_{k=0}^n$ is an orthonormal basis of $\mathcal{V}_n$. As a basis of Π_n, we order $\{\widetilde{\varphi}_{n,k}\}$ lexicographically based on the ordering in (3.4) and (3.3),

$$\{\widetilde{\varphi}_\ell\}_{\ell=1}^N = \{\widetilde{\varphi}_{0,0}, \widetilde{\varphi}_{1,0}, \widetilde{\varphi}_{1,1}, \widetilde{\varphi}_{2,0}, \ldots, \widetilde{\varphi}_{n,0}, \ldots, \widetilde{\varphi}_{n,n}\}.$$

Returning to (3.1), we define

$$\widetilde{\psi}_{n,k}(x,y) = \left(1 - x^2 - y^2\right)\widetilde{\varphi}_{n,k}(x,y)$$

for the Dirichlet case and

$$\widetilde{\psi}_{n,k}(x,y) = \widetilde{\varphi}_{n,k}(x,y)$$

in the Neumann case. To calculate the first order partial derivatives of $\widetilde{\psi}_{n,k}(x,y)$, we need $U_n'(t)$. The values of $U_n(t)$ and $U_n'(t)$ are evaluated using the standard triple recursion relations,

$$\begin{aligned} U_{n+1}(t) &= 2tU_n(t) - U_{n-1}(t), \\ U_{n+1}'(t) &= 2U_n(t) + 2tU_n'(t) - U_{n-1}'(t). \end{aligned}$$

ETNA
Kent State University
http://etna.math.kent.edu

For the numerical approximation of the integrals in (3.2), which are over B being the unit disk, we use the formula

$$\int_B g(x,y)\,dx\,dy \approx \sum_{l=0}^{q}\sum_{m=0}^{2q} g\left(r_l, \frac{2\pi\, m}{2q+1}\right)\omega_l \frac{2\pi}{2q+1} r_l. \tag{3.5}$$

Here the numbers ω_l are the weights of the $(q+1)$-point Gauss-Legendre quadrature formula on $[0,1]$. Note that

$$\int_0^1 p(x)dx = \sum_{l=0}^{q} p(r_l)\omega_l,$$

for all single-variable polynomials $p(x)$ with $\deg(p) \le 2q+1$. The formula (3.5) uses the trapezoidal rule with $2q+1$ subdivisions for the integration over $\overline{B}$ in the azimuthal variable. This quadrature (3.5) is exact for all polynomials $g \in \Pi_{2q}$. This formula is also the basis of the hyperinterpolation formula discussed in [18].

3.2. The three–dimensional case. In $\mathbb{R}^3$, the dimension of Π_n is

$$N_n = \binom{n+3}{3} = \frac{1}{6}(n+1)(n+2)(n+3).$$

Here we choose orthonormal polynomials on the unit ball as described in [14],

$$\begin{aligned}\widetilde{\varphi}_{m,j,\beta}(\mathbf{x}) &= c_{m,j} p_j^{(0,m-2j+\frac{1}{2})}(2\|\mathbf{x}\|^2-1) S_{\beta,m-2j}\left(\frac{\mathbf{x}}{\|\mathbf{x}\|}\right)\\ &= c_{m,j}\|\mathbf{x}\|^{m-2j} p_j^{(0,m-2j+\frac{1}{2})}(2\|\mathbf{x}\|^2-1) S_{\beta,m-2j}\left(\frac{\mathbf{x}}{\|\mathbf{x}\|}\right), \qquad (3.6)\\ j &= 0,\dots,\lfloor m/2\rfloor, \quad \beta = 0,1,\dots,2(m-2j), \quad m = 0,1,\dots,n. \qquad (3.7)\end{aligned}$$

Here $c_{m,j} = 2^{\frac{5}{4}+\frac{m}{2}-j}$ is a constant, and $p_j^{(0,m-2j+\frac{1}{2})}$, $j \in \mathbb{N}_0$, are the normalized Jabobi polynomials which are orthonormal on $[-1,1]$ with respect to the inner product,

$$(v,w) = \int_{-1}^{1} (1+t)^{m-2j+\frac{1}{2}} v(t) w(t)\, dt;$$

see for example [1, 16]. The functions $S_{\beta,m-2j}$ are spherical harmonic functions and they are given in spherical coordinates by

$$S_{\beta,k}(\phi,\theta) = \widetilde{c}_{\beta,k}\begin{cases}\cos(\frac{\beta}{2}\phi) T_k^{\frac{\beta}{2}}(\cos\theta), & \beta \text{ even},\\ \sin(\frac{\beta+1}{2}\phi) T_k^{\frac{\beta+1}{2}}(\cos\theta), & \beta \text{ odd}.\end{cases}$$

The constant $\widetilde{c}_{\beta,k}$ is chosen in such a way that the functions are orthonormal on the unit sphere S^2 in $\mathbb{R}^3$,

$$\int_{S^2} S_{\beta,k}(\mathbf{x})\, S_{\widetilde{\beta},\widetilde{k}}(\mathbf{x})\, dS = \delta_{\beta,\widetilde{\beta}}\,\delta_{k,\widetilde{k}}.$$

The functions T_k^l are the associated Legendre polynomials; see [19, 23]. According to (3.1), we define the basis for our space of trial functions by

$$\widetilde{\psi}_{m,j,\beta}(\mathbf{x}) = (1-\|\mathbf{x}\|^2)\widetilde{\varphi}_{m,j,\beta}(\mathbf{x})$$

ETNA
Kent State University
http://etna.math.kent.edu

in the Dirichlet case and by

$$\widetilde{\psi}_{m,j,\beta}(\mathbf{x}) = \widetilde{\varphi}_{m,j,\beta}(\mathbf{x})$$

in the Neumann case We can order the basis lexicographically. To calculate all of the above functions we can use recursive algorithms similar to the one used for the Chebyshev polynomials. These algorithms also allow the calculation of the derivatives of each of these functions; see [16, 30].

For the numerical approximation of the integrals in (3.2), we use a quadrature formula for the unit ball B,

$$\int_B g(\mathbf{x})\,d\mathbf{x} = \int_0^1 \int_0^{2\pi} \int_0^{\pi} \widetilde{g}(r,\theta,\phi)\, r^2 \sin(\phi)\, d\phi\, d\theta\, dr \approx Q_q[g],$$
$$Q_q[g] := \sum_{i=1}^{2q} \sum_{j=1}^{q} \sum_{k=1}^{q} \frac{\pi}{q}\,\omega_j\,\nu_k \widetilde{g}\left(\frac{\zeta_k+1}{2}, \frac{\pi\, i}{2q}, \arccos(\xi_j)\right).$$

Here $\widetilde{g}(r,\theta,\phi) = g(\mathbf{x})$ is the representation of g in spherical coordinates. For the θ integration we use the trapezoidal rule, because the function is $2\pi-$periodic in θ. For the r direction we use the transformation

$$\begin{aligned}\int_0^1 r^2 v(r)\, dr &= \int_{-1}^1 \left(\frac{t+1}{2}\right)^2 v\left(\frac{t+1}{2}\right)\frac{dt}{2} \\ &= \frac{1}{8}\int_{-1}^1 (t+1)^2 v\left(\frac{t+1}{2}\right)\, dt \\ &\approx \sum_{k=1}^{q} \underbrace{\frac{1}{8}\nu_k'}_{=:\nu_k} v\left(\frac{\zeta_k+1}{2}\right),\end{aligned}$$

where the ν_k' and ζ_k are the weights and the nodes of the Gauss quadrature with q nodes on $[-1,1]$ with respect to the inner product

$$(v,w) = \int_{-1}^1 (1+t)^2 v(t) w(t)\, dt.$$

The weights and nodes also depend on q but we omit this index. For the ϕ direction we use the transformation

$$\int_0^{\pi} \sin(\phi) v(\phi)\, d\phi = \int_{-1}^1 v(\arccos(\phi))\, d\phi \approx \sum_{j=1}^{q} \omega_j v(\arccos(\xi_j)),$$

where the ω_j and ξ_j are the nodes and weights for the Gauss–Legendre quadrature on $[-1,1]$. For more information on this quadrature rule on the unit ball in $\mathbb{R}^3$, see [27].

Finally we need the gradient in Cartesian coordinates to approximate the integral in (3.2), but the function $\widetilde{\varphi}_{m,j,\beta}(\mathbf{x})$ in (3.6) is given in spherical coordinates. Here we simply use the chain rule, with $\mathbf{x} = (x,y,z)$,

$$\begin{aligned}\frac{\partial}{\partial \mathbf{x}} v(r,\theta,\phi) = \frac{\partial}{\partial r} v(r,\theta,\phi)\cos(\theta)\sin(\phi) - \frac{\partial}{\partial \theta} v(r,\theta,\phi)\frac{\sin(\theta)}{r\sin(\phi)} \\ + \frac{\partial}{\partial \phi} v(r,\theta,\phi)\frac{\cos(\theta)\cos(\phi)}{r},\end{aligned}$$

and similarly for $\frac{\partial}{\partial y}$ and $\frac{\partial}{\partial z}$.

ETNA
Kent State University
http://etna.math.kent.edu

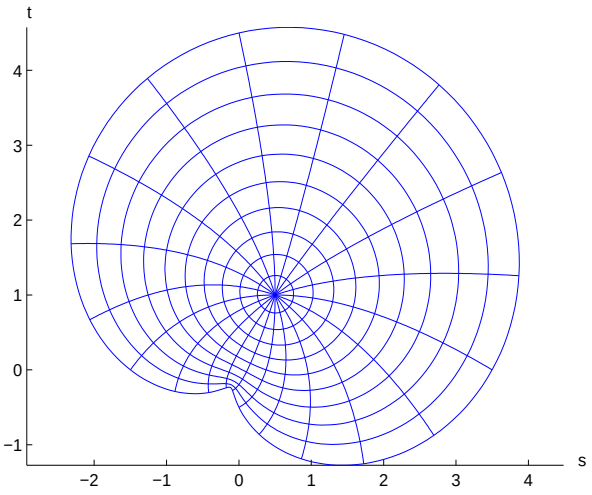

FIG. 4.1. *The 'limacon' region (4.3)-(4.4).*

4. Numerical examples. Our programs are written in MATLAB. Some of the examples we give are so chosen that we can invert explicitly the mapping Φ, to be able to better construct our test examples. Having a knowledge of an explicit inverse for Φ is not needed when applying the method; but it can simplify the construction of test cases. In other test cases, we have started from a boundary mapping $\varphi : \partial B_d \xrightarrow[onto]{1-1} \partial\Omega$ and have generated a smooth mapping $\Phi : \overline{B}_d \xrightarrow[onto]{1-1} \overline{\Omega}$.

The problem of generating such a mapping Φ when given only φ is often quite difficult. In some cases, a suitable definition for Φ is straightforward. For example, the ellipse

$$\varphi(\cos\theta, \sin\theta) = (a\cos\theta, b\sin\theta), \qquad 0 \le \theta \le 2\pi,$$

has the following simple extension to the unit disk B_2,

$$\Phi(x, y) = (ax, by), \qquad (x, y) \in \overline{B}_2. \tag{4.1}$$

In general, however, the construction of Φ when given only φ is non-trivial. For the plane, we can always use a conformal mapping; but this is too often non-trivial to construct. In addition, conformal mappings are often more complicated than are needed. For example, the simple mapping (4.1) is sufficient for our applications, whereas the conformal mapping of the unit disk onto the ellipse is much more complicated; see [7, Sec. 5].

We have developed a variety of numerical methods to generate a suitable Φ when given the boundary mapping φ. The topic is too complicated to consider in any significant detail in this paper and it will be the subject of a forthcoming paper. However, to demonstrate that our algorithms for generating such extensions Φ do exist, we give examples of such Φ in the following examples that illustrate our spectral method.

4.1. The planar Dirichlet problem. We begin by illustrating the numerical solution of the eigenvalue problem,

$$\begin{aligned} Lu(\mathbf{s}) \equiv -\Delta u = \lambda u(\mathbf{s}), \qquad & \mathbf{s} \in \Omega \subseteq \mathbb{R}^2, \\ u(\mathbf{s}) \equiv 0, \qquad & \mathbf{s} \in \partial\Omega. \end{aligned} \tag{4.2}$$

ETNA
Kent State University
http://etna.math.kent.edu

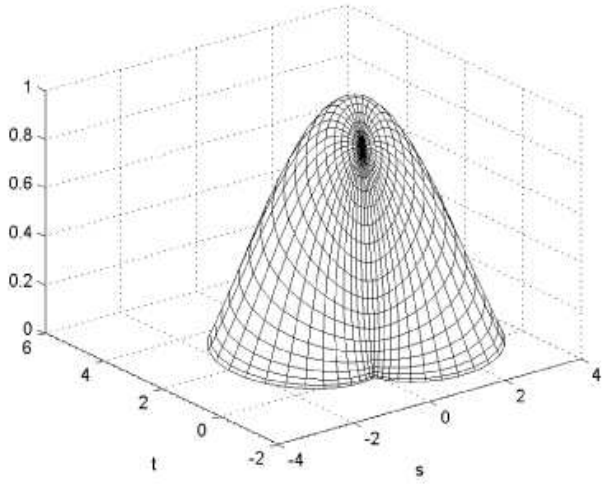

FIG. 4.2. *Eigenfunction for the limacon boundary corresponding to the approximate eigenvalue* $\lambda^{(1)} \doteq 0.68442$.

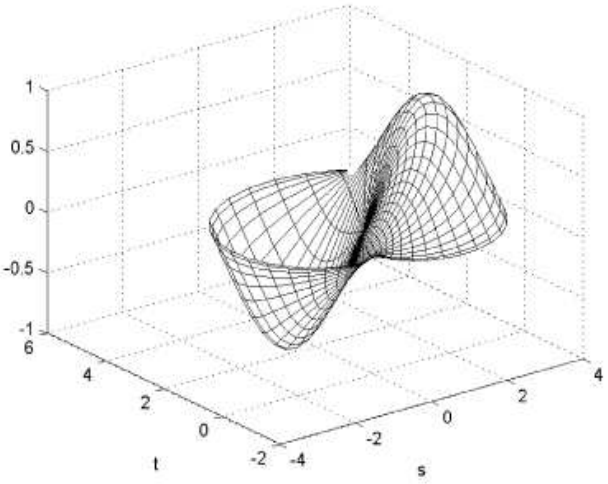

FIG. 4.3. *Eigenfunction for the limacon boundary corresponding to the approximate eigenvalue* $\lambda^{(2)} \doteq 1.56598$.

This corresponds to choosing $A = I$ in the framework presented earlier. Thus, we need to calculate

$$\widetilde{A}(\mathbf{x}) = J(\mathbf{x})^{-1} J(\mathbf{x})^{-\mathrm{T}}.$$

For our variables, we replace a point $\mathbf{x} \in B_2$ with (x, y), and we replace a point $\mathbf{s} \in \Omega$ with (s, t). The boundary $\partial\Omega$ is a generalized limacon boundary defined by

$$\varphi(\cos\theta, \sin\theta) = (p_3 + p_1 \cos\theta + p_2 \sin\theta)(a\cos\theta, b\sin\theta), \quad 0 \le \theta \le 2\pi. \tag{4.3}$$

ETNA
Kent State University
http://etna.math.kent.edu

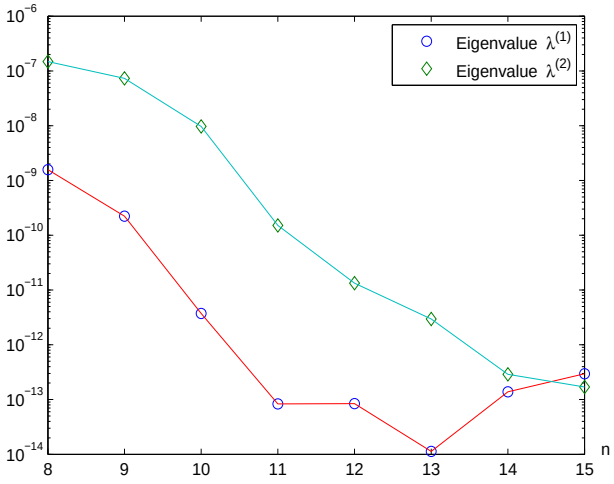

FIG. 4.4. *The values of* $\left|\lambda_{n+1}^{(k)} - \lambda_n^{(k)}\right|$ *for* $k = 1, 2$ *for increasing degree* n.

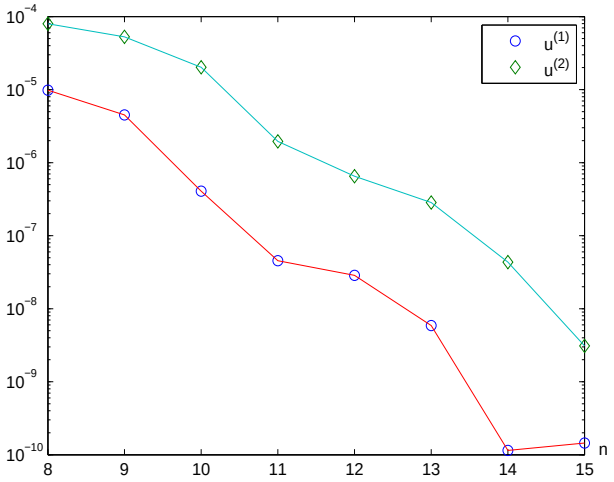

FIG. 4.5. *The values of* $\|u_{n+1}^{(k)} - u_n^{(k)}\|_\infty$ *for* $k = 1, 2$ *for increasing degree* n.

The constants a, b are positive numbers, and the constants $\mathbf{p} = (p_1, p_2, p_3)$ must satisfy

$$p_3 > \sqrt{p_1^2 + p_2^2}.$$

The mapping $\Phi : \overline{B}_2 \rightarrow \overline{\Omega}$ is given by $(s, t) = \Phi(x, y)$ with both components s and t being polynomials in (x, y). For our numerical example, each component of $\Phi(x, y)$ is a polynomial of degree 2 in (x, y). We use the particular parameters

$$(a, b) = (1, 1), \quad \mathbf{p} = (1.0, 2.0, 2.5). \tag{4.4}$$

ETNA
Kent State University
http://etna.math.kent.edu

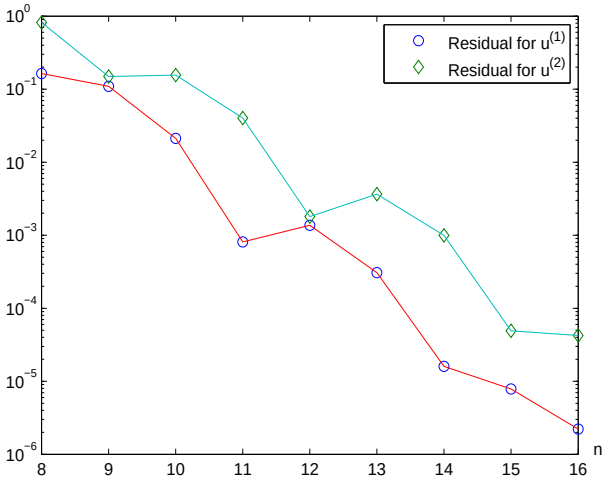

FIG. 4.6. *The values of* $\|R_n^{(k)}\|_\infty$ *for* $k = 1, 2$ *for increasing degree* n.

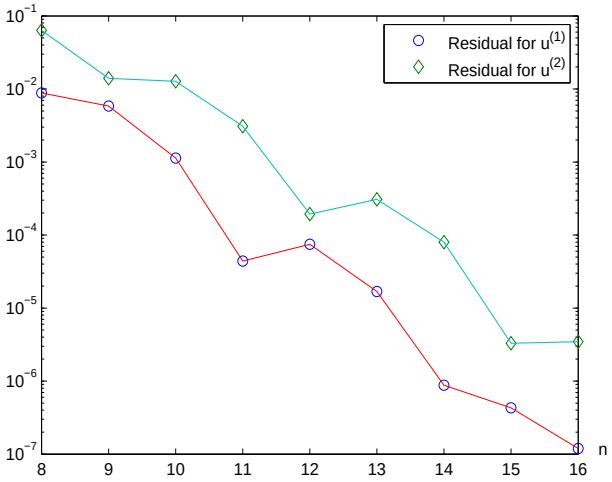

FIG. 4.7. *The values of* $\|R_n^{(k)}\|_2$ *for* $k = 1, 2$ *for increasing degree* n.

In Figure 4.1, we give the images in $\overline{\Omega}$ of the circles, $r = j/10$, $j = 0, 1, \ldots, 10$, and the azimuthal lines, $\theta = j\pi/10$, $j = 1, \ldots, 20$. Our generated mapping Φ maps the origin $(0, 0)$ to a more centralized point inside the region.

As a sidenote, the straightforward generalization of (4.3),

$$\Phi(x, y) = (p_3 + p_1 x + p_2 y)(ax, by), \qquad (x, y) \in B_2,$$

does not work. It is neither 1-1 nor onto. Also, the mapping

$$\Phi(r\cos\theta, r\sin\theta) = (p_3 + p_1\cos\theta + p_2\sin\theta)(ar\cos\theta, br\sin\theta)$$

ETNA
Kent State University
http://etna.math.kent.edu

does not work because it is not differentiable at the origin, $(x, y) = (0, 0)$.

Figures 4.2 and 4.3 give the approximate eigenfunctions for the two smallest eigenvalues of (4.2) over our limacon region. Because the true eigenfunctions and eigenvalues are unknown for almost all cases (with the unit ball as an exception), we used other methods for studying experimentally the rate of convergence. Let $\lambda_n^{(k)}$ denote the value of the k^{th} eigenvalue based on the degree n polynomial approximation, with the eigenvalues taken in increasing order. Let $u_n^{(k)}$ denote a corresponding eigenfunction,

$$\widetilde{u}_n^{(k)}(\mathbf{x}) = \sum_{j=1}^{N_n} \alpha_j^{(n)} \widetilde{\psi}_j(\mathbf{x}),$$

with $\alpha^{(n)} \equiv \left[\alpha_1^{(n)}, \ldots, \alpha_N^{(n)}\right]$, the eigenvector of (3.2) associated with the eigenvalue $\lambda_n^{(k)}$. We normalize the eigenfunctions by requiring $\|u_n^{(k)}\|_\infty = 1$. Define

$$\Lambda_n = \left|\lambda_{n+1}^{(k)} - \lambda_n^{(k)}\right|, \qquad D_n = \|u_{n+1}^{(k)} - u_n^{(k)}\|_\infty.$$

Figures 4.4 and 4.5 show the decrease, respectively, of Λ_n and D_n as n increases. In both cases, we use a semi-log scale. Also, consider the residual,

$$R_n^{(k)} = -\Delta u_n^{(k)} - \lambda_n^{(k)} u_n^{(k)},$$

with the Laplacian $\Delta u_n^{(k)}$ computed analytically. Figures 4.6 and 4.7 show the decrease of $\|R_n^{(k)}\|_\infty$ and $\|R_n^{(k)}\|_2$, respectively, again on a semi-log scale. Note that the L^2-norm of the residual is significantly smaller than the maximum norm. When looking at a graph of $R_n^{(k)}$, it is small over most of the region Ω, but it is more badly behaved when (x, y) is near to the point on the boundary that is nearly an inverted corner.

These numerical results all indicate an exponential rate of convergence for the approximations $\left\{\lambda_n^{(k)} : n \geq 1\right\}$ and $\left\{u_n^{(k)} : n \geq 1\right\}$ as a function of the degree n. In Figure 4.4, the maximum accuracy for $\lambda^{(1)}$ appears to have been found with the degree $n = 13$, approximately. For larger degrees, rounding errors dominate. We also see that the accuracy for the first eigenvalue-eigenfunction pair is better than that for the second such pair. This pattern continues as the eigenvalues increase in size, although a significant number of the leading eigenvalues remain fairly accurate, enough for practical purposes. For example,

$$\lambda_{16}^{(10)} - \lambda_{15}^{(10)} \doteq 2.55 \times 10^{-7},$$
$$\left\|u_{16}^{(10)} - u_{15}^{(10)}\right\|_\infty \doteq 1.49 \times 10^{-4}.$$

We also give an example with a more badly behaved boundary, namely,

$$\varphi(\cos\theta, \sin\theta) = (5 + \sin\theta + \sin 3\theta - \cos 5\theta)(\cos\theta, \sin\theta), \qquad 0 \leq \theta \leq 2\pi, \tag{4.5}$$

to which we refer as an 'amoeba' boundary. We create a function $\Phi : \overline{B}_2 \xrightarrow[onto]{1-1} \overline{\Omega}$; the mapping is pictured in Figure 4.8 in the manner analogous to that done in Figure 4.1 for the limacon boundary. Both components of $\Phi(x, y)$ are polynomials in (x, y) of degree 6. As discussed earlier, we defer to a future paper a discussion of the construction of Φ; the method was different than that used for the limacon boundary. In Figure 4.9, we give an approximation to the eigenfunction corresponding to the eigenvalue, $\lambda^{(2)} \doteq 0.60086$. The approximation uses a polynomial approximation of degree $n = 30$. For it, we have

$$\|R_{30}^{(2)}\|_\infty \doteq 0.730, \qquad \|R_{30}^{(2)}\|_2 \doteq 0.0255.$$

ETNA
Kent State University
http://etna.math.kent.edu

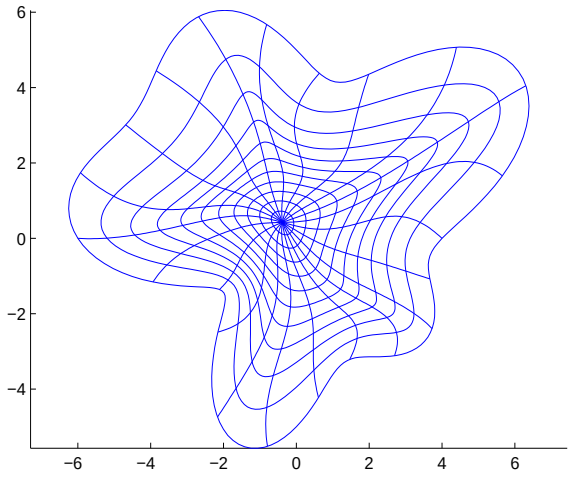

FIG. 4.8. *An 'amoeba' region with boundary (4.5).*

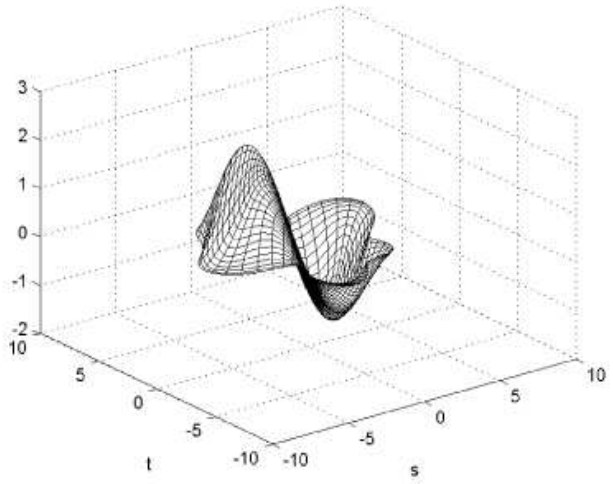

FIG. 4.9. *Eigenfunction for the amoeba boundary corresponding to the approximate eigenvalue* $\lambda^{(2)} \doteq 0.60086$.

4.2. Comparison using alternative trial functions. To ensure that our method does not lead to poor convergence properties when compared to traditional spectral methods, we compare in this section our use of polynomials over the unit disk to some standard trial functions used with traditional spectral methods. We picked two sets of trial functions that are presented in [10, Sec. 18.5].

The first choice is the shifted Chebyshev polynomials with a quadratic argument,

$$\text{(4.6)} \qquad \begin{cases} \sin(m\theta)T_j(2r^2-1), & \cos(m\theta)T_j(2r^2-1), & m \text{ even}, \\ \sin(m\theta)rT_j(2r^2-1), & \cos(m\theta)rT_j(2r^2-1), & m \text{ odd}, \end{cases} \qquad j = 0, 1, \ldots,$$

where $m \in \mathbb{N}_0$; the sine terms with $m = 0$ are omitted. These functions are not smooth on

ETNA
Kent State University
http://etna.math.kent.edu

TABLE 4.1
Function enumerations.

		n odd		
$\cos(0\theta)$	$\widetilde{T}_1^E(r)$ **(1)**	$\widetilde{T}_2^E(r)$ **(3)**	$\widetilde{T}_3^E(r)$ **(7)**	$\widetilde{T}_4^E(r)$ **(13)**
$\cos(1\theta)$	$\widetilde{T}_1^O(r)$ **(5)**	$\widetilde{T}_2^O(r)$ **(9)**	$\widetilde{T}_3^O(r)$ **(15)**	$\dots$
$\cos(2\theta)$	$\widetilde{T}_1^E(r)$ **(11)**	$\widetilde{T}_2^E(r)$ **(17)**	$\dots$	
$\cos(3\theta)$	$\widetilde{T}_1^O(r)$ **(19)**	$\dots$		
		n even		
$\sin(1\theta)$	$\widetilde{T}_1^O(r)$ **(2)**	$\widetilde{T}_2^O(r)$ **(4)**	$\widetilde{T}_3^O(r)$ **(8)**	$\widetilde{T}_4^O(r)$ **(14)**
$\sin(2\theta)$	$\widetilde{T}_1^E(r)$ **(6)**	$\widetilde{T}_2^E(r)$ **(10)**	$\widetilde{T}_3^E(r)$ **(16)**	$\dots$
$\sin(3\theta)$	$\widetilde{T}_1^O(r)$ **(12)**	$\widetilde{T}_2^O(r)$ **(18)**	$\dots$	
$\sin(4\theta)$	$\widetilde{T}_1^E(r)$ **(20)**	$\dots$		

the unit disk. Also, to ensure that the functions satisfy the boundary condition for $r = 1$, we use

$$\widetilde{T}_j^E(r) \equiv T_j\left(2r^2 - 1\right) - 1 \quad \text{and} \quad \widetilde{T}_j^O(r) \equiv rT_j(2r^2 - 1) - r, \qquad j = 1, 2, \dots,$$

instead of the radial functions given in (4.6). Because these functions are not polynomials, the notion of degree does not make sense. To compare these functions to the ridge polynomials we have to enumerate them so we can use the same number of trial functions in our comparison. The result is a sequence of trial functions $\widetilde{\varphi}_k^C$, $k \in \mathbb{N}$. If k is even, we use a sine term; and if k is odd, we use a cosine term. Then we use a triangular scheme to enumerate the function according to Table 4.1. This Table implies, for example, that

$$\widetilde{\varphi}_{15}^C(\theta, r) = \cos(\theta)\widetilde{T}_3^O(r),$$
$$\widetilde{\varphi}_{10}^C(\theta, r) = \sin(2\theta)\widetilde{T}_2^E(r).$$

As a consequence of the triangular scheme, we use relatively more basis functions with lower frequencies.

As a second set of trial functions, we chose the 'one-sided Jacobi polynomials', given by

$$\begin{cases} \sin(m\theta)\, r^m P_j^{0,m}(2r^2 - 1), & m = 1, 2, \dots, \quad j = 0, 1, \dots, \\ \cos(m\theta)\, r^m P_j^{0,m}(2r^2 - 1), & m = 0, 1, \dots, \quad j = 0, 1, \dots, \end{cases} \tag{4.7}$$

where the $P_j^{0,m}$ are the Jacobi polynomials of degree j. These trial functions are smooth on the unit disk; and in order to satisfy the boundary condition at $r = 1$, we use

$$\widetilde{P}_j^{0,m}(r) := P_j^{0,m}(2r^2 - 1) - 1, \qquad j = 1, 2, \dots,$$

instead of the radial functions in (4.7). We use an enumeration scheme analogous to that given in Table 4.1. The result is a sequence of trial functions $\widetilde{\varphi}_k^J$, $k \in \mathbb{N}$. For example,

$$\widetilde{\varphi}_{15}^J(\theta, r) = \cos(\theta)\, r\widetilde{P}_3^{0,1}(r),$$
$$\widetilde{\varphi}_{10}^J(\theta, r) = \sin(2\theta)\, r^2\widetilde{P}_2^{0,2}(r).$$

When we compare the different trial functions in the following we always label the horizontal axis with n, and this implies that N_n trial functions are used.

ETNA
Kent State University
http://etna.math.kent.edu

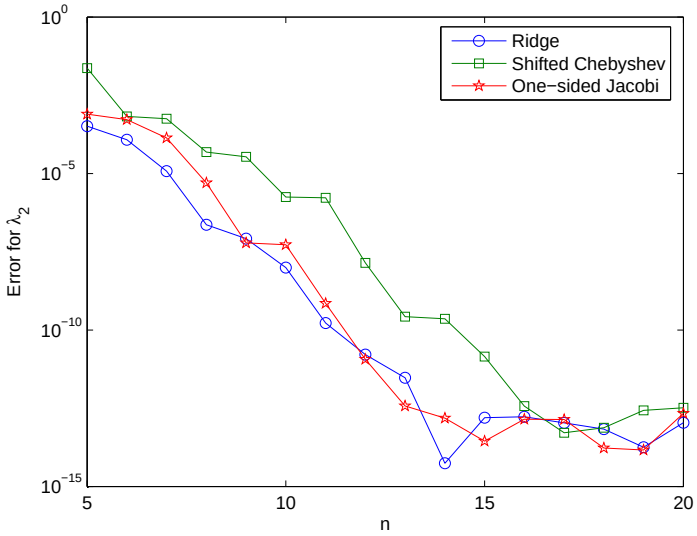

FIG. 4.10. *Errors* $\left|\lambda^{(2)} - \lambda_n^{(2)}\right|$ *for the three different sets of trial functions.*

For our comparison, we used the same problem (4.2) with the region shown in Figure 4.1. We have chosen to look at the convergence for the second eigenvalue $\lambda^{(2)}$, and we plot errors for the eigenvalue itself and the norms of the residuals, $\| - \Delta u_n^{(2)} - \lambda_n^{(2)} u_n^{(2)}\|_2$ and $\| - \Delta u_n^{(2)} - \lambda_n^{(2)} u_n^{(2)}\|_\infty$; see Figures 4.10–4.11. All three figures show that for each set of trial functions the rate of convergence is exponential for this example. Also in each figure the ridge and the one-sided Jacobi polynomials show a faster convergence than the shifted Chebyshev polynomials. For the convergence of the eigenvalue approximation there seems to be no clear difference between the ridge and the one-sided Jacobi polynomials. For the norm of the residual the one-sided Jacobi polynomials seem to be slightly better for larger n. The same tendency was also visible for $\lambda^{(1)}$, but was not as clear. We conclude that the ridge polynomials are a good choice.

Because of the requirement of using polar coordinates for traditional spectral methods and the resulting changes to the partial differential equation, we find that the implementation is easier with our method. For a complete comparison, however, we would need to look at the most efficient way to implement each method, including comparing operation counts for the competing methods.

4.3. The three-dimensional Neumann problem. We illustrate our method in $\mathbb{R}^3$, doing so for the Neumann problem. We use two different domains. Let B_3 denote the closed unit ball in $\mathbb{R}^3$. The domain $\Omega_1 = \Phi_1(B_3)$ is given by

$$\mathbf{s} = \Phi_1(\mathbf{x}) \equiv \begin{pmatrix} x_1 - 3x_2 \\ 2x_1 + x_2 \\ x_1 + x_2 + x_3 \end{pmatrix},$$

so B_3 is transformed to an ellipsoid Ω_1; see Figure 4.13. The domain Ω_2 is given by

$$\Phi_2 \begin{pmatrix} \rho \\ \phi \\ \theta \end{pmatrix} = \begin{pmatrix} (1 - t(\rho))\rho + t(\rho)T(\phi, \theta) \\ \phi \\ \theta \end{pmatrix}, \tag{4.8}$$

ETNA
Kent State University
http://etna.math.kent.edu

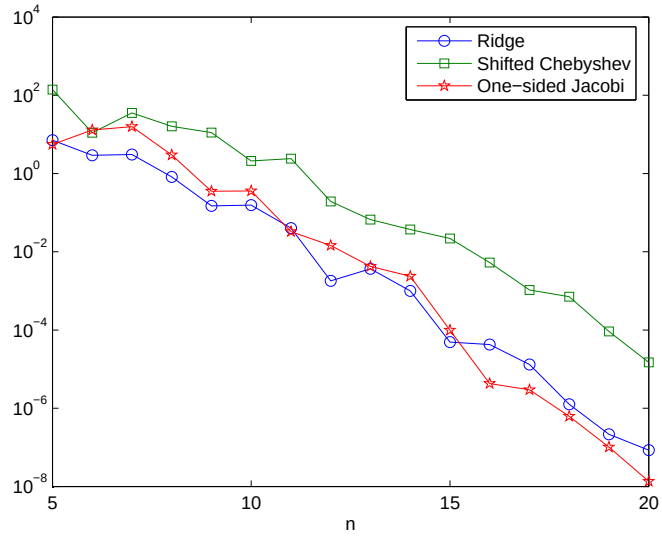

FIG. 4.11. *The residual* $\|\Delta u_n^{(2)} + \lambda_n^{(2)} u_n^{(2)}\|_\infty$ *for the three different sets of trial functions.*

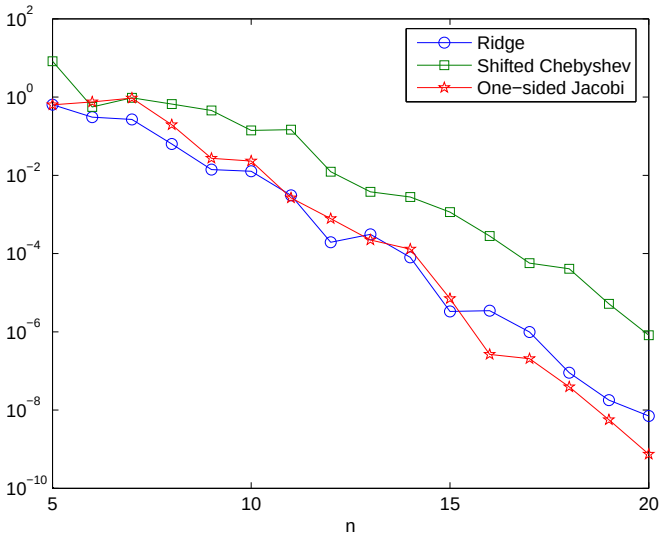

FIG. 4.12. *The residual* $\|\Delta u_n^{(2)} + \lambda_n^{(2)} u_n^{(2)}\|_2$ *for the three different sets of trial functions.*

where we used spherical coordinates $(\rho, \phi, \theta) \in [0,1] \times [0, 2\pi] \times [0, \pi]$ to define the mapping Φ_2. Here the function $T : S^2 = \partial B_3 \mapsto (1, \infty)$ is a function which determines the boundary of a star shaped domain Ω_2. The restriction $T(\phi, \theta) > 1$ guarantees that Φ_2 is injective, and this can always be assumed after a suitable scaling of Ω_2. For our numerical example, we use

$$T(\theta, \phi) = 2 + \frac{3}{4}\cos(2\phi)\sin(\theta)^2(7\cos(\theta)^2 - 1).$$

ETNA
Kent State University
http://etna.math.kent.edu

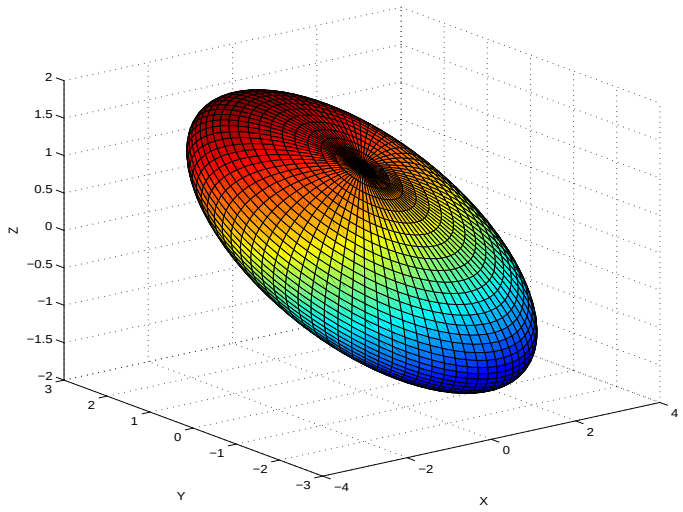

FIG. 4.13. *The boundary of* Ω_1.

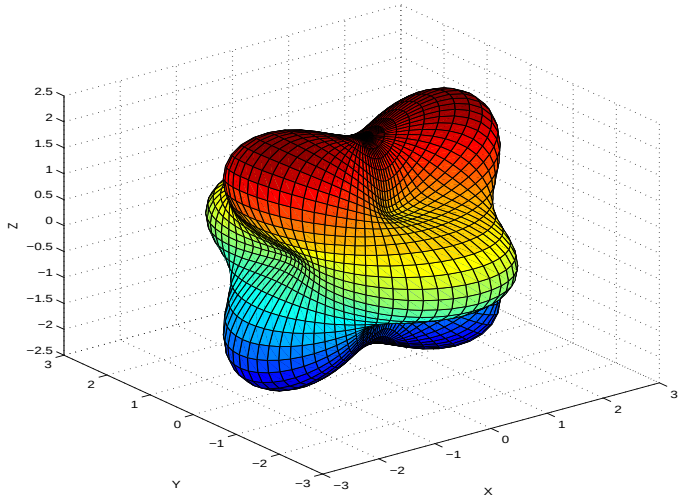

FIG. 4.14. *A view of* $\partial\Omega_2$.

Finally, the function t is defined by

$$t(\rho) \equiv \begin{cases} 0, & 0 \le \rho \le \frac{1}{2}, \\ 2^5(\rho - \frac{1}{2})^5, & \frac{1}{2} < \rho \le 1, \end{cases}$$

where the exponent 5 implies $\Phi_2 \in C^4(B_1(0))$. See [6] for a more detailed description of Φ_2; one perspective of the surface Ω_2 is shown in Figure 4.14.

For each domain we calculate the approximate eigenvalues $\lambda_n^{(i)}$, $\lambda_n^{(0)} = 0 < \lambda_n^{(1)} \le$

ETNA
Kent State University
http://etna.math.kent.edu

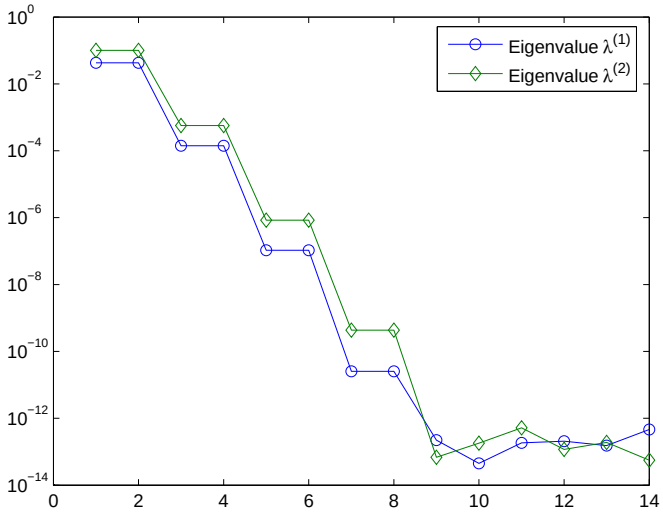

FIG. 4.15. Ω_1: *errors* $\left|\lambda_{15}^{(i)} - \lambda_n^{(i)}\right|$ *for the calculation of the first two eigenvalues* $\lambda^{(i)}$.

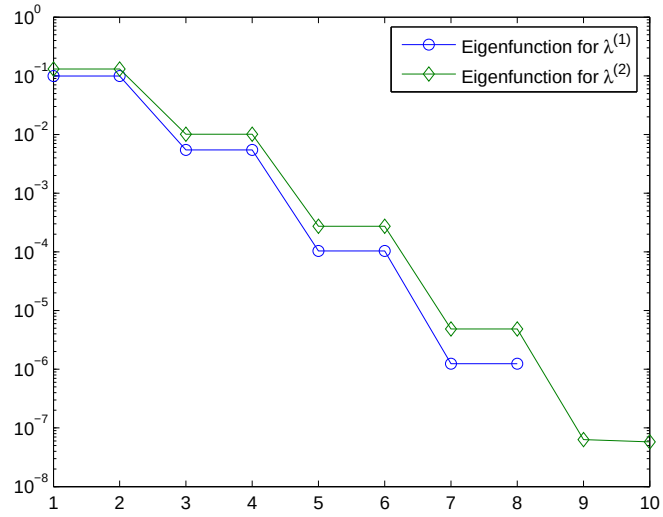

FIG. 4.16. Ω_1: *angles* $\angle\left(u_n^{(i)}, u_{15}^{(i)}\right)$ *between the approximate eigenfunction* $u_n^{(i)}$ *and our most accurate approximation* $u_{15}^{(i)} \approx u^{(i)}$.

$\lambda_n^{(2)} \leq \ldots$ and eigenfunctions $u_n^{(i)}$, $i = 1, \ldots, N_n$, for the degrees $n = 1, \ldots, 15$ (here we do not indicate dependence on the domain Ω). To analyze the convergence we calculate several numbers. First, we estimate the speed of convergence for the first two eigenvalues by calculating $|\lambda_{15}^{(i)} - \lambda_n^{(i)}|$, $i = 1, 2$, $n = 1, \ldots, 14$. Then to estimate the speed of convergence of the eigenfunctions we calculate the angle (in $L^2(\Omega)$) between the current approximation

ETNA
Kent State University
http://etna.math.kent.edu

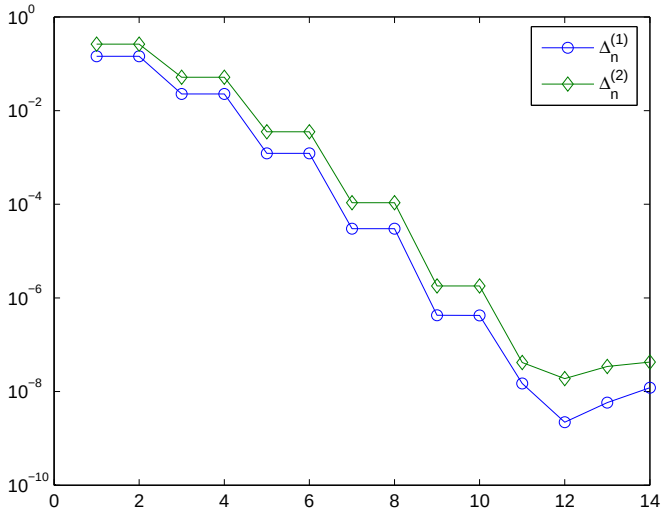

FIG. 4.17. Ω_1: *errors* $\left|-\Delta u_n^{(i)}(s) - \lambda_n^{(i)} u_n^{(i)}(s)\right|$.

and the most accurate approximation $\angle(u_n^{(i)}, u_{15}^{(i)})$, $i = 1, 2$, $n = 1, \ldots, 14$. Finally, an independent estimate of the quality of our approximation is given by

$$R_n^{(i)} \equiv |-\Delta u_n^{(i)}(\mathbf{s}) - \lambda_n^{(i)} u(\mathbf{s})|,$$

where we use only one $\mathbf{s} \in \Omega$, given by $\Phi(1/10, 1/10, 1/10)$. We approximate $\Delta u_n^{(i)}(\mathbf{s})$ numerically as the analytic calculation of the second derivatives of $u_n^{(i)}(\mathbf{s})$ is quite complicated. To approximate the Laplace operator we use a second order difference scheme with $h = 0.0001$ for Ω_1 and $h = 0.01$ for Ω_2. The reason for the latter choice of h is that our approximations for the eigenfunctions on Ω_2 are only accurate up three to four digits, so if we divide by h^2 the discretization errors are magnified to the order of 1.

The graphs in Figures 4.15–4.17, seem to indicate exponential convergence. For the graphs of $\angle(u_n^{(i)}, u_{15}^{(i)})$, see Figure 4.16. We remark that we use the function $\arccos(x)$ to calculate the angle, and for $n \approx 9$ the numerical calculations give $x = 1$, so the calculated angle becomes 0. For the approximation of $R_n^{(i)}$ one has to remember that we use a difference method of order $O(h^2)$ to approximate the Laplace operator, so we can not expect any result better than 10^{-8} if we use $h = 0.0001$.

As we expect, the approximations for Ω_2 with the transformation Φ_2 present a bigger problem for our method. Still from the graphs in Figure 4.18 and 4.19 we might infer that the convergence is exponential, but with a smaller exponent than for Ω_1. Because $\Phi_2 \in C^4(B_3)$ we know that the transformed eigenfunctions on B_3 are in general only C^4, so we can only expect a convergence of $O(n^{-4})$. The values of n which we use are too small to show what we believe is the true behavior of the $R_n^{(i)}$, although the values for $n = 10, \ldots, 14$ seem to indicate some convergence of the type we would expect.

The poorer convergence for Ω_2 as compared to Ω_1 illustrates a general problem. When defining a surface $\partial\Omega$ by giving it as the image of a 1-1 mapping φ from the unit sphere S^2 into $\mathbb{R}^3$, how does one extend it to a smooth mapping Φ from the unit ball to Ω? The mapping in (4.8) is smooth, but it has large changes in its derivatives, and this affects the rate

ETNA
Kent State University
http://etna.math.kent.edu

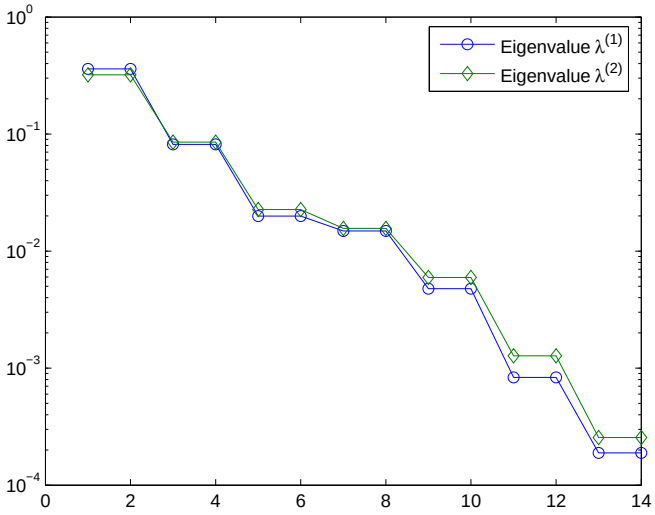

FIG. 4.18. Ω_2: *errors* $\left|\lambda_{15}^{(i)} - \lambda_n^{(i)}\right|$ *for the calculation of the first two eigenvalues* $\lambda^{(i)}$.

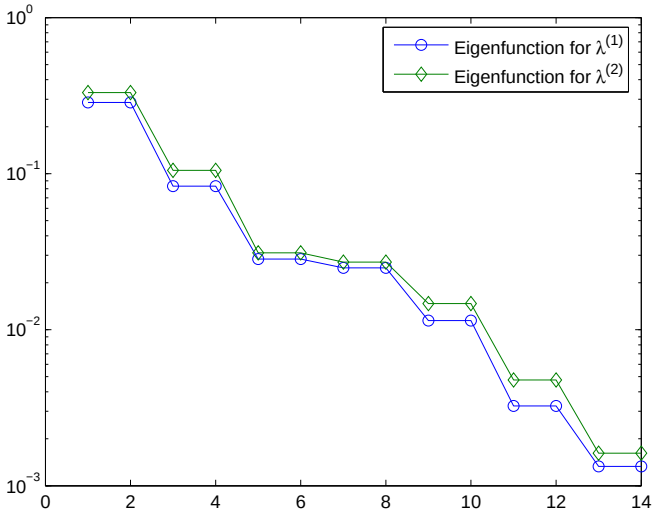

FIG. 4.19. Ω_2: *angles* $\angle\left(u_n^{(i)}, u_{15}^{(i)}\right)$ *between the approximate eigenfunction* $u_n^{(i)}$ *and our most accurate approximation* $u_{15}^{(i)} \approx u^{(i)}$.

of convergence of our spectral method. As was discussed at the beginning of this section, we are developing a toolkit of numerical methods for generating such functions Φ. This will be developed in detail in a future paper.

ETNA
Kent State University
http://etna.math.kent.edu

REFERENCES

[1] M. ABRAMOWITZ AND I. A. STEGUN, *Handbook of Mathematical Functions*, Dover, New York, 1965.
[2] K. ATKINSON, *The numerical solution of the eigenvalue problem for compact integral operators*, Trans. Amer. Math. Soc., 129 (1967), pp. 458–465.
[3] ———, *Convergence rates for approximate eigenvalues of compact integral operators*, SIAM J. Numer. Anal., 12 (1975), pp. 213–222.
[4] ———, *The Numerical Solution of Integral Equations of the Second Kind*, Cambridge University Press, Cambridge, 1997.
[5] K. ATKINSON, D. CHIEN, AND O. HANSEN, *A spectral method for elliptic equations: The Dirichlet problem*, Adv. Comput. Math., 33 (2010), pp. 169–189.
[6] K. ATKINSON, O. HANSEN, AND D. CHIEN, *A spectral method for elliptic equations: The Neumann problem*, Adv. Comput. Math., DOI=10.1007/s10444-010-9154-3, to appear.
[7] K. ATKINSON AND W. HAN, *On the numerical solution of some semilinear elliptic problems*, Electron. Trans. Numer. Anal., 17 (2004), pp. 206–217. http://etna.math.kent.edu/vol.17.2004/pp206-217.dir.
[8] K. ATKINSON AND W. HAN, *Theoretical Numerical Analysis: A Functional Analysis Framework*, Third ed., Springer, New York, 2009.
[9] T. BAGBY, L. BOS, AND N. LEVENBERG, *Multivariate simultaneous approximation*, Constr. Approx., 18 (2002), pp. 569–577.
[10] J. BOYD, *Chebyshev and Fourier Spectral Methods*, Second ed., Dover, New York, 2000.
[11] C. CANUTO, A. QUARTERONI, MY. HUSSAINI, AND T. ZANG, *Spectral Methods in Fluid Mechanics*, Springer, New York, 1988.
[12] ———, *Spectral Methods - Fundamentals in Single Domains*, Springer, New York, 2006.
[13] F. CHATELIN, *Spectral Approximation of Linear Operators*, Academic Press, New York, 1983.
[14] C. DUNKL AND Y. XU, *Orthogonal Polynomials of Several Variables*, Cambridge University Press, Cambridge, 2001.
[15] L. EVANS, *Partial Differential Equations*, American Mathematical Society, Providence, RI, 1998.
[16] W. GAUTSCHI, *Orthogonal Polynomials*, Oxford University Press, Oxford, 2004.
[17] D. GOTTLIEB AND S. ORSZAG, *Numerical Analysis of Spectral methods: Theory and Applications*, SIAM, Philadlphia, 1977.
[18] O. HANSEN, K. ATKINSON, AND D. CHIEN, *On the norm of the hyperinterpolation operator on the unit disk and its use for the solution of the nonlinear Poisson equation*, IMA J. Numer. Anal., 29 (2009), pp. 257–283.
[19] E. W. HOBSON, *The Theory of Spherical and Ellipsoidal Harmonics*, Chelsea Publishing, New York, 1965.
[20] M. KRASNOSELSKII, *Topological Methods in the Theory of Nonlinear Integral Equations*, Pergamon Press, Oxford, 1964.
[21] O. LADYZHENSKAYA AND N. URALT'SEVA, *Linear and Quasilinear Elliptic Equations*, Academic Press, New York, 1973.
[22] B. LOGAN. AND L. SHEPP, *Optimal reconstruction of a function from its projections*, Duke Math. J., 42 (1975), pp. 645–659.
[23] T. M. MACROBERT, *Spherical Harmonics*, Dover, New York, 1948.
[24] J. OSBORN, *Spectral approximation for compact operators*, Math. Comp., 29 (1975), pp. 712–725.
[25] D. RAGOZIN, *Constructive polynomial approximation on spheres and projective spaces*, Trans. Amer. Math. Soc., 162 (1971), pp. 157–170.
[26] J. SHEN AND T. TANG, *Spectral and High-Order Methods with Applications*, Science Press, Beijing, 2006.
[27] A. STROUD, *Approximate Calculation of Multiple Integrals*, Prentice-Hall, Englewood Cliffs, NJ, 1971.
[28] H. TRIEBEL, *Higher Analysis*, Hüthig, Heidelberg, 1997.
[29] YUAN XU, *Lecture notes on orthogonal polynomials of several variables*, in Advances in the Theory of Special Functions and Orthogonal Polynomials, Nova Science Publishers, Hauppauge, NY, 2004, pp. 135–188.
[30] S. ZHANG AND J. JIN, *Computation of Special Functions*, John Wiley & Sons, Inc., New York, 1996.